Published in final edited form as:
J Huntingtons Dis. 2013 June 18; 2(1): 201–215. doi:10.3233/JHD-130058.

The de-ubiquitinating enzyme ataxin-3 does not modulate disease progression in a knock-in mouse model of Huntington disease

Li Zeng[1], **Sara J. Tallaksen-Greene**[1], **Bo Wang**[1], **Roger L. Albin**[1,2], and **Henry L. Paulson**[1,*]
[1]Department of Neurology, University of Michigan, Ann Arbor, MI, USA
[2]Geriatrics Research, Education, and Clinical Center, VAAAHS, Ann Arbor, MI, USA

Abstract

Ataxin-3 is a deubiquitinating enzyme (DUB) that participates in ubiquitin-dependent protein quality control pathways and, based on studies in model systems, may be neuroprotective against toxic polyglutamine proteins such as the Huntington's disease (HD) protein, huntingtin (htt). HD is one of at least nine polyglutamine neurodegenerative diseases in which disease-causing proteins accumulate in ubiquitin-positive inclusions within neurons. In studies crossing mice null for ataxin-3 to an established HD knock-in mouse model (HdhQ200), we tested whether loss of ataxin-3 alters disease progression, perhaps by impairing the clearance of mutant htt or the ubiquitination of inclusions. While loss of ataxin-3 mildly exacerbated age-dependent motor deficits, it did not alter inclusion formation, ubiquitination of inclusions or levels of mutant or normal htt. Ataxin-3, itself a polyglutamine-containing protein with multiple ubiquitin binding domains, was not observed to localize to htt inclusions. Changes in neurotransmitter receptor binding known to occur in HD knock-in mice also were not altered by the loss of ataxin-3, although we unexpectedly observed increased $GABA_A$ receptor binding in the striatum of HdhQ200 mice, which has not previously been noted. Finally, we confirmed that CNS levels of hsp70 are decreased in HD mice as has been reported in other HD mouse models, regardless of the presence or absence of ataxin-3. We conclude that while ataxin-3 may participate in protein quality control pathways, it does not critically regulate the handling of mutant htt or contribute to major features of disease pathogenesis in HD.

Keywords

Ataxin-3; Huntington disease; ubiquitin-proteasome pathway; Neurodegenerative disease; polyglutamine

Introduction

Huntington's disease (HD) is one of at least nine polyglutamine neurodegenerative diseases caused by an abnormally long polyglutamine (polyQ) tract in the disease protein, which in HD is Huntingtin (htt) [1]. PolyQ expansion favors abnormal conformations in the disease protein leading to protein misfolding and aggregation. A common neuropathological hallmark in HD and other polyglutamine diseases is the accumulation of ubiquitin-positive

* Corresponding author. Address: Department of Neurology, University of Michigan, 109 Zina Pitcher Place, BSRB Room 4188, Ann Arbor, MI 48109, USA. Tel.: +17346156156; Fax: +17346155655; henryp@umich.edu.

Conflict of Interest
The authors have no conflict of interest to declare.

inclusions in the nucleus, soma and distal processes of neurons [2, 3]. In HD, neurodegeneration preferentially occurs in the striatum and cortex but ultimately is observed throughout the brain [4].

Two main pathways are responsible for the clearance of misfolded proteins, the ubiquitin-proteasome pathway (UPP) and the autophagy-lysosome system. The UPP predominantly degrades short-lived and misfolded proteins while the autophagylysosome system handles larger protein complexes and organelles [5]. Several UPP components are known to affect the ubiquitination, degradation or toxicity of mutant htt [6]. For example, the ubiquitin-conjugating enzyme E2-25K interacts with htt [7], induces mutant htt aggregation and promotes cell death [8]. The E3 ubiquitin ligase Hrd1 enhances degradation of mutant htt and suppresses mutant htt toxicity in cells [9], and another E3, parkin, has been reported to colocalize with mutant htt in HD brain and reduce levels of mutant htt [10]. A third E3, C-terminus of Hsp70-interacting protein (CHIP), plays dual roles in the UPP and molecular chaperone systems that together suppress htt neurotoxicity in vitro and in vivo[11]. These results demonstrate that the UPP pathway is critical to the clearance of mutant htt.

Several lines of evidence suggest that the deubiquitinating enzyme ataxin-3, itself a polyglutamine disease protein causing Spinocerebellar ataxia type 3 (SCA3), also functions in the UPP to counter the accumulation and toxicity of polyglutamine disease proteins like htt. Ataxin-3 is a specialized deubiquitinating enzyme (DUB) implicated in ubiquitin-dependent protein quality control [12-15]. Studies to date suggest ataxin-3 is a neuroprotective protein by virtue of its ubiquitin-linked functions [16]. It interacts with numerous E3 ubiquitin ligases including CHIP [17-19] and parkin [19] in vitro and in cells. It preferentially cleaves longer polyubiquitin chains [12, 13, 20], and participates in delivering misfolded proteins to the proteasome for degradation [21]. It also regulates aggresome formation in cell models [22]. Overexpression of human ataxin-3 in Drosophila suppresses neurodegeneration caused by mutant htt in a manner that is dependent on its ubiquitin-associated functions [23]. Conversely, deletion of ataxin-3 results in lower levels of hsp70 in fibroblasts and mouse brain [24] and in the accumulation of ubiquitinated proteins in brain [25]. Finally, knocking down ataxin-3 with RNAi leads to disorganization of the cytoskeleton and induces cell death in human and mouse cell lines[26]. Many of these results were obtained in cell systems or with overexpressed ataxin-3. Whether these putative cytoprotective actions of ataxin-3 play a significant role in countering polyglutamine toxicity in the CNS under more physiological conditions, however has not been determined.

To assess the putative neuroprotective function of ataxin-3 against polyglutamine toxicity, we tested whether loss of ataxin-3 alters the disease phenotype in a mouse model of HD. We used an established HD knock-in model (HdhQ200) that expresses a ~200 repeat expansion in the murine homologue of htt and displays a progressive HD-like behavioral and neuropathologic phenotype [27]. We crossed HdhQ200 mice with knock-out mice lacking ataxin-3. While genetic deletion of ataxin-3 modestly aggravated motor dysfunction in HdhQ200 mice, the loss of ataxin-3 did not worsen the accumulation of htt and inclusions or other phenotypic features in HdhQ200 mice. In addition, we confirm an earlier observation [28] that Hsp70 levels are decreased in the brain of HD mice and report that $GABA_A$ receptor binding is increased in the striatum of 60-week-old HdhQ200 mice regardless of the presence or absence of ataxin-3. Our results suggest that while ataxin-3 may participate in protein quality control, is not a critical modulator of HD disease pathogenesis.

Materials and methods

Mouse strains

Heterozygous HdhQ200 mice [27] were bred to *Atxn3* knock-out mice [24] to generate heterozygous HdhQ200/*Atxn3* haploinsufficient mice (HdhQ200/Atxn3$^{+/-}$). The F1 progeny were then bred to *Atxn3* knock-out mice or wild-type mice to obtain F2 generation HdhQ200 heterozygous mice with no or two ataxin-3 alleles (HdhQ200/Atxn3$^{-/-}$ or HdhQ200/Atxn3$^{+/+}$). All animals were housed and handled in accordance with the NIH Guide for the Care and Use of Laboratory Animals. All animals were housed in a specific pathogenic-free condition with a 12h light/dark cycle maintained at 23 °C.

Genotyping and CAG repeat size determination

All mice were genotyped as follows. DNA was extracted from a 0.5 cm mouse tail with DNeasy Blood & Tissue Kit (Qiagen, Valencia, CA). HdhQ200 knock-in mice were identified using the following primer sequences: forward primer CCCATTCATTGCCTTGCTG; and reverse primer GCGGCTGAGGGGGTTGA. PCR amplification was performed using LA Taq with GC buffer II (Takara Bio Inc). PCR conditions were as follows: 98 °C for 5 min, followed by 30 cycles at 98 °C for 30 s, 53 °C for 30 s, 72 °C for 1.5 min, and a final extension at 72 °C for 5 min.

The forward primer sequence designed to identify the *Atxn3* knock-out allele was: AAATGGCGTTACTTAAGCTAG. The forward primer sequence used to identify the wild type allele was: GAGGGAAGTCGTCATAAGAGT. The common reverse primer was: TGGGCTACAAGAAATCCTGTC. PCR amplification was performed using a LA Taq with GC buffer I (Takara Bio Inc). PCR conditions were as follows: 98 °C for 3 min, followed by 30 cycles at 96 °C for 30 s, 55 °C for 45 s, 72 °C for 1 min, and a final extension at 72 °C for 5 min.

DNA products were separated by standard 1.5 % agarose gel electrophoresis and visualized with ethidium bromide using a Gel Doc system (Bio Rad). DNA samples were also sent to Laragen (Laragen Inc., Los Angeles, CA, USA) to determine the CAG repeat number. HdhQ200 mutant alleles ranged from 190 to 220 CAG repeats.

Weight and Balance Beam measurement

The balance beam apparatus [27, 29] consists of two elevated plastic platforms, horizontally 50 cm above a table. The start platform is light and open, while the finishing platform is a darkened enclosed box.

Progressive motor dysfunction was evaluated by assessing the ability to cross 11 mm round and 5 mm square beams to reach the dark safety platform. Seven time points were assessed: 10, 20, 30, 40, 50, 63 and 70 weeks of age. At each time point, a total of 4 days of behavioral trials with two trials each day was performed for both beams. Time to cross each beam was recorded for each trial with a 20 s maximum cutoff. If the mouse fell from the beam, it was scored as 20 s. The first three days of trials were for acclimation and the last two trials were analyzed as testing trials. Mice were weighed on the first day at each time point.

10-11 animals were assessed for HdhQ200/Atxn3$^{+/+}$ and HdhQ200/Atxn3$^{-/-}$ groups, and 5-6 animals were assessed for WT/Atxn3$^{+/+}$ and WT/Atxn3$^{-/-}$ groups. Animals were euthanized at 75 weeks for pathologic examination. All behavioral evaluations were performed with the examiner blinded to genotype.

Brain tissue harvesting

Mice were anesthetized with an intraperitoneal injection of ketamine/xylazine mixture and perfused transcardially with 0.1 M phosphate buffer. Brains were dissected and divided sagittally into two halves. One half was quickly frozen at -80°C for biochemical studies. The other half was immersion fixed in 4% paraformaldehyde at 4°C for 24 hours, cryoprotected in 30% sucrose in 0.1 M phosphate buffer for an additional 24 hours at 4°C. This fixed hemisphere was used for immunohistochemical analysis.

Western blot analysis

Flash-frozen brains were homogenized in RIPA buffer (50 mM Tris, 150 mM NaCl, 0.1% SDS, 0.5% deoxycholic acid, 1% Nonidet P-40, pH 7.4) with Complete Mini Protease Inhibitor tablets (Roche). After sonication and centrifugation, supernatants were supplemented with 1% final SDS and 100 mM DTT, boiled and loaded on SDS-PAGE and transferred to polyvinylidene difluoride membranes. Unless otherwise mentioned, 10% acrylamide SDS-PAGE was used. For certain experiments, because of the high molecular weight of htt (~350 kDa), we employed a modified SDS-PAGE in which the top half of the separating gel is 6% acrylamide, poured over a solidified bottom half of 10% acrylamide.

Membranes were blocked for 30 min in blocking buffer (TBS-Tween with 5% skim milk), then incubated overnight with primary antibodies at 4°C. The following antibodies were used: mouse anti-polyQ 1C2 (1:10,000; Millipore, Billerica, MA, USA), mouse anti-htt 2166 (1:500; Millipore), rabbit anti-tubulin-α (1:10,000; Cell signaling), mouse anti-ataxin-3 1H9 (1:1000; Millipore), rabbit anti-ubiquitin (1:5000; Dako, Denmark) and mouse anti-Hsp70 (1:1000; Enzo). For secondary antibodies, peroxidase-conjugated goat anti-mouse or goat anti-rabbit secondary antibody (1:10,000; Jackson Immunoresearch) was incubated with membranes for 1 hour at room temperature. Blots were developed using blue basic autorad films (GeneMate). ImageJ software was used for semi-quantification of band intensities.

Immunohistochemistry

Immunohistochemical labeling was performed as described previously [29, 30]. Briefly, hemispheres fixed in 4% paraformaldehyde were sectioned at 30 μm sagittally through the entire hemisphere. Free-floating sections were labeled the following primary antibodies: Goat anti N-terminal htt (1:250; Santa Cruz Biotechnology, Santa Cruz, CA, USA), mouse anti-ataxin-3 1H9 antibody (1:500; Millipore), rabbit anti-ubiquitin (1:500; Dako). Immunoreactivity was obtained using the Vectastain Elite Kit (Vector Laboratories, Burlingame, CA) according to the manufacturer's protocol. Sections were developed in ImmPACT DAB (Vector Laboratories), mounted on Superfrost slides (Fisher Scientific, Pittsburgh, PA) and air dried after dehydration with graded ethanol and xylene. Coverslips were affixed with DPX (Electron Microscopy Sciences, Hatfield, PA, USA). All sections were imaged with an Olympus digital microscope. The images were processed using Photoshop CS2 to generate the figures without changing the balance or contrast.

Quantification of neuronal inclusion bodies

Neuronal inclusion bodies were quantified on sagittal sections immunohistochemically labeled with anti N-terminal htt. Digital images chosen randomly by an individual blinded to genotype were taken with a x100 lens (Olympus BX51 microscope). Three or four sections per region per animal were analyzed with the Image Processing Toolbox in Matlab (R2011b, Mathworks) to determine the size and numbers of inclusion bodies. The numbers of inclusions were averaged and expressed as total number per image (4080x3072 pixels), and the size of inclusions were shown as mean pixels/inclusion.

Quantitative receptor autoradiography

60-week-old mice were used for receptor autoradiography analysis (n=4/group). Brains were extracted immediately after decapitation and divided sagittally. After coating with M1 embedding matrix (Thermo scientific), brains were frozen on dry ice and stored at -80°C.

Autoradiographic studies were performed as described previously [27, 29]. Brains were serially cut in 15 μm sections at -12°C, mounted on Superfrost slides and stored at -80°C until use. For D1 dopamine receptors assays, sections were incubated in 25 mM Tris, 100 mM NaCl, 1 mM $MgCl_2$, 0.001% ascorbic acid, and 1 μM pargyline, pH 7.2, with radioactive ligand 0.55 nM [^{3}H]SCH23390 (Amersham Biosciences, Cardiff, UK) (Specific activity 84 Ci/mmol) for 2.5 hours at room temperature. Nonspecific binding was determined in the presence of 1 μM cis-flupenthixol.

For D2 dopamine receptors assays, sections were incubated in 25 mM Tris, 100 mM NaCl, 1 mM $MgCl_2$, 0.001% ascorbic acid, and 1 μM pargyline, pH 7.2, with 0.75 nM [^{3}H]Spiperone (Amersham Biosciences) (Specific activity 81 Ci/mmol) with 100 nM mianserin for 2.5 hours. Nonspecific binding was determined in the presence of 50 μM dopamine.

For $GABA_A$/benzodiazepine receptors assay, slides were incubated in 50 mM Tris-citrate buffer, pH 7.2, with 5 nM [^{3}H]flunitrazepam (DuPont Biotechnology systems, Wilmington, DE) (Specific activity 85 Ci/mmol) for 1 hour at 4 °C. Nonspecific binding was determined in ligand buffer with 2 μM clonazepam.

Slides and ^{14}C standards (ARC, St Louis, MO, USA) were arrayed in a standard x-ray cassette, and an autoradiogram was generated by direct apposition of the tissue to the emulsion side of a tritium imaging plate (BSA-TR2025; Fuji Photo Film, Japan) for 8 hours. Autoradiograms were analyzed by quantitative densitometry using an MCID-M2 image analysis system (Interfocus Ltd, England). Optical density (OD) measurements were made for each section in which the structure was visible, sampling as large an area as possible. Specific binding was determined by subtracting non-specific binding from the total binding.

Statistical analyses

All statistical analyses were carried out using Prism (Graphpad, La Jolla, CA). One-way ANOVA with post hoc comparisons or two-paired *t*-test was applied to compare different groups (between genotypes). While two-way ANOVA was performed on experiments for behavioral tests. There were no interactions observed between genotype and training. Results are presented as mean ± SEM. Significant differences were accepted when $p<0.05$.

Results

Generation of HdhQ200/Atxn3$^{+/+}$ and HdhQ200/Atxn3$^{-/-}$ mice

To determine whether endogenous ataxin-3 plays an important role in countering the neurotoxic effects of mutant htt, we crossed HdhQ200 mice to *Atxn3* knock-out mice to generate four genotypes: HdhQ200/Atxn3$^{+/+}$, HdhQ200/Atxn3$^{-/-}$, WT/Atxn3$^{+/+}$ and WT/Atxn3$^{-/-}$. PCR was employed to confirm the genotypes of mice (Fig. 1A), and DNA samples were sent to Laragen Inc. for CAG repeat length determination. Mean size analysis demonstrated that the HdhQ200 mutant allele ranged from 190 to 220 CAG repeats, with no significant difference in CAG repeat size between HdhQ200/Atxn3$^{+/+}$ and HdhQ200/Atxn3$^{-/-}$ in both male and female mice (male, $p=0.1857$; female, $p=0.1610$) (Fig. 1B).

Loss of ataxin-3 modestly exacerbates behavioral phenotype in HdhQ200 mice

Ataxin-3 is presumed to protect broadly against the toxic effects of misfolded proteins [23, 31]. We analyzed the effect of deleting endogenous ataxin-3 on the phenotype of HdhQ200 mice. Body weight measurements at different time points showed a significant weight loss in HdhQ200 male and female mice by 50 wks, but deletion of ataxin-3 had no significant effect on weight changes in males and females. (Fig. 1C-D). We also evaluated the effect of ataxin-3 deletion on motor performance, as measured by balance beam analysis, which has been used effectively to characterize motor deficits in HdhQ200 mouse model [27]. Deletion of ataxin-3 significantly increased ($p < 0.05$) the latency to cross 11 mm round beam in HdhQ200 mice at age 63 weeks and exacerbated ($p < 0.05$) the performance on 5 mm square beam in HdhQ200 mice at age 50 and 63 weeks (Fig. 1E-F). By age 70 weeks, however, HdhQ200 mice were so impaired that most mice could not cross beams in 20 s, whether with or without ataxin-3. Thus, the presence of ataxin-3 may modestly mitigate aspects of htt toxicity that are responsible for worsened motor performance of HdhQ200 mice as they age.

Deletion of ataxin-3 does not alter neurotransmitter receptor changes observed in HdhQ200 mice

Expression levels of dopamine D1 and D2 decline sharply over the course of disease in human HD patients as well as transgenic and knock-in mouse models of HD [27, 29, 32, 33]. Changes in D1 and D2 receptors both contribute to dysfunctional signaling in HD brain [33]. To determine whether the absence of ataxin-3 exacerbated the loss of dopamine D1 and D2 receptors, we performed quantitative receptor autoradiography at age 60 weeks, a time when motor deficits are pronounced. As expected, and confirming previous reports [27] 60-week-old HdhQ200 mice exhibited a significant decrease in dopamine D1 binding in the striatum, nuclear accumbens (nAcc) and olfactory tubercle (Olf Tub) (Fig. 2A-B). A similar decrease in dopamine D2 binding was also observed in HdhQ200 mice (data not shown). We also assessed $GABA_A$ receptor binding to survey neuronal integrity in diverse brain regions. Intriguingly, 60-week-old HdhQ200 mice showed a significant increase in striatal $GABA_A$ receptor binding (Fig. 2C-D). No difference in $GABA_A$ receptor binding was observed in any other brain region between genotypes (Fig. 2D). In contrast, previous results from 80-week-old HdhQ200 mice showed normal levels of $GABA_A$ receptor binding in striatum [27]. For all three neurotransmitter receptors, the presence or absence of ataxin-3 did not significantly alter the changes in binding observed in HdhQ200 versus wild type mice (Fig. 2).

Loss of ataxin-3 does not alter levels of mutant htt or normal htt in HdhQ200 mice

We next sought to determine whether endogenous ataxin-3 altered the steady state level of mutant or normal htt proteins. Western blot was used to measure htt protein levels in forebrains of all four genotypes at different ages. Probing with 1C2 antibody, which selectively binds expanded polyglutamine, revealed full length expanded htt (~350 KDa) and its proteolytic fragments in HdhQ200 mice whereas no detectable proteins were observed in WT mice on either an ataxin-$3^{+/+}$ or ataxin-$3^{-/-}$ background (Fig. 3A). Analysis of band densities showed that the average 1C2 immunoreactivity in HdhQ200/Atxn$3^{+/+}$ versus HdhQ200/Atxn$3^{-/-}$ brain at different time points did not differ significantly (Fig. 3C). We next used htt-2166 antibody which recognizes both normal and expanded htt to evaluate the protein levels of htt at 45 and 75 weeks old. Identical findings were obtained: the band densities of expanded htt or normal htt in HdhQ200/Atxn$3^{+/+}$ versus HdhQ200/Atxn$3^{-/-}$ were indistinguishable (Fig. 3B, E-F). Thus, two different antibodies used to evaluate htt levels in HdhQ200 brain at different time points showed no significant differences in the presence or absence of ataxin-3.

Loss of ataxin-3 does not alter inclusion body formation

Inclusion bodies are a pathological marker of HD. To determine whether the modestly worsened motor deficit in HdhQ200/Atxn3$^{-/-}$ mice correlated with changes in the size or density of inclusion bodies, we performed immunohistochemistry with an N-terminal htt antibody on brain sections from 19, 45 and 75 weeks old mice. As expected, WT/ Atxn3$^{+/+}$ and WT/ Atxn3$^{-/-}$ did not exhibit any htt-positive inclusions anywhere (Fig. 4). In HdhQ200 mice as previously reported inclusions were absent at 19 weeks but appeared widely in striatum, cortex, hippocampus and cerebellum at 45 weeks in HdhQ200 mice [27]. Inclusions further increased in size and amount at 75 weeks of age. Analysis of the number and size of inclusion bodies in defined brain regions showed no difference between HdhQ200/Atxn3$^{+/+}$ and HdhQ200/Atxn3$^{-/-}$ mice (Table 1A-D). In summary, these results indicate that loss of ataxin-3 does not significantly alter the density or size of htt inclusions or the time course of their formation in HdhQ200 mice.

Deletion of ataxin-3 does not alter ubiquitination of inclusions, but increases total ubiquitinated proteins in the CNS of wild type and HdhQ200 mice

Although deletion of ataxin-3 did not enhance inclusion body formation, genetic deletion of ataxin-3 conceivably could alter the ubiquitination of inclusions since ataxin-3 is a DUB. To test this possibility, immunohistochemistry with anti-ubiquitin antibody was performed on brain sections from 75-week-old mice. We analyzed four brain regions (striatum, cortex, hippocampus and cerebellum) to ensure a thorough comparison of ubiquitination between genotypes. Comparison of ubiquitinated inclusions in HdhQ200 mice revealed no obvious difference in the ubiquitination of inclusions in the presence or absence of ataxin-3 (Fig. 5A). Identical findings were also noted in 45-week-old mice (data not shown). Interestingly, western blot of total forebrain homogenates probed with ubiquitin antibody showed upregulation of total ubiquitinated proteins in *Atxn3* knockout mice, as has been described [25], regardless of htt genotype (Fig. 5B-C). Compared to WT mice, the increase of total RIPA-soluble ubiquitinated proteins in HdhQ200 mice only showed a trend towards statistical significance ($p>0.05$). These results suggest that despite ataxin-3's function as a DUB, it does not appreciably modulate the ubiquitination of htt inclusions, even though it does appear to modulate the ubiquitination of other proteins.

Ataxin-3 is not detectably recruited into htt inclusions

Previous work has demonstrated prominant localization of overexpressed ataxin-3 to polyQ inclusion bodies in Drosophila [23], and ataxin-3 colocalizes to the intranuclear inclusions known as Marinesco bodies in aged human brain [34, 35]. To test whether endogenous murine ataxin-3 similarly localizes to htt inclusions, we performed immunohistochemistry with 1H9 antibody on brain sections from 45 week old HdhQ200 mice, an age when htt inclusions are abundant and easily detectable (Fig. 6). In SCA3 knock-in mice expressing polyglutamine-expanded murine ataxin-3, 1H9 antibody robustly immunostains intranuclear inclusions in striatal neurons (data not shown), establishing that this antibody is able to visualize endogenous ataxin-3 in inclusions. In HdhQ200 mice, however, we failed to observe immunostaining of inclusions with 1H9 antibody: htt inclusions showed similar negative 1H9 immunostaining whether ataxin-3 was present or absent in the mouse. In HdhQ200 mice as in wild type mice, endogenous ataxin-3 immunostaining remained diffuse throughout the cytoplasm. Ataxin-3 has been reported to concentrate in the nucleus under certain cellular stressors [36] but we did not observe a shift of ataxin-3 immunostaining into the nuclei of neurons. Although negative ataxin-3 immunostaining of inclusions does not rule out the possibility of low levels of ataxin-3 within inclusions, we conclude that the subcellular distribution of ataxin-3 in neurons is not markedly altered by the presence of aggregating htt in HD mice.

Hsp70 levels are decreased in HD mice but are not further altered by loss of ataxin-3

Ataxin-3 has been reported to regulate basal and stress-induced levels of hsp70 [24], and mutant htt impairs the heat shock response in cell and mouse models, including hsp70 induction [37]. To investigate whether ataxin-3 alters hsp70 levels in response to polyQ-induced toxicity, we used western blot to measure hsp70 levels in the brains of all tested genotypes at 45 and 75 weeks of age. As was previously reported in another HD mouse model [28], a decrease in hsp70 levels was observed in HdhQ200 mice compared to WT mice (Fig. 7). We failed, however, to observe any difference in the levels of hsp70 between HdhQ200/Atxn3$^{+/+}$ and HdhQ200/Atxn3$^{-/-}$ at either age (Fig. 7). Therefore, ataxin-3 does not appear to regulate hsp70 expression levels in HdhQ200 mice.

Discussion

Based on ataxin-3's well established ubiquitin-linked activities and previous work supporting a protective function for this protein against polyQ neurotoxicity in a Drosophila model, we hypothesized that loss of ataxin-3 would exacerbate polyQ toxicity in the HdhQ200 model. In contrast to our expectations, however, deletion of the murine *Atxn3* gene resulted in only mild, transient exacerbation of motor dysfunction and failed to alter other aspects of disease including levels of mutant htt, inclusion formation and striatal dopamine receptor expression. Our findings suggest that caution should be exercised in interpreting prior studies as indicating a significant protective function of ataxin-3 in Huntington's disease. Similar results from a SAC3 transgenic mouse model [38] and a rat model of Machado-Joseph disease [39] also fail to support a robust neuroprotective function of ataxin-3 in polyglutamine-induced neurodegeneration. It is possible that one or more of the three other DUBs belonging to the same Josephin domain-containing DUB family as ataxin-3 plays similar roles to ataxin-3 and compensates for its absence in *Atxn3* knock-out models [16, 40-42]. To more directly assess the protective function of ataxin-3, it might be necessary to simultaneously disable one or more of the other JosD family proteins. Alternatively, ataxin-3 could be overexpressed in HD knock-in mice to further address the putative neuroprotective function of ataxin-3 in HD pathogenesis.

In addition to its DUB activity, ataxin-3 is also reported to bind DNA and interact with transcription regulators [43-45]. Heat shock or oxidative stress drive ataxin-3 into the nucleus where it may regulate transcription of specific genes such as manganese superoxide dismutase(SOD2) [46]. Ataxin-3 also modulates basal and stress-induced hsp70 transcription, with loss of ataxin-3 leading to a decrease in hsp70 levels in brain tissue [24]. An important molecular chaperone, hsp70 promotes the ATP-dependent renaturation of misfolded proteins [47]. Consistent with this function, genetic deletion of hsp70 exacerbates pathogenesis of HD disease in R6/2 transgenic mouse model [48]. Progressive decrease in chaperone protein levels has been observed in HD cell and mouse models [28, 37]. We hypothesized that loss of ataxin-3 would exacerbate the phenotype of HD disease by decreasing the expression of hsp70. Our results, however, indicate that ataxin-3 fails to alter the decrease of hsp70 in HdhQ200 mice.

The HdhQ200 knock-in mouse model, which expresses a mutated murine homologue of huntingtin, exhibits more slowly progressive behavioral dysfunction and neuropathologic features than most transgenic models of HD [49, 50]. Knock-in mice with the expanded allele accumulate polyQ protein inclusions as early as 20 weeks and as disease progresses, HdhQ200 mice show progressive motor impairments on the balance beam starting at 50 weeks accompanied by remarkable reduction in striatal dopamine receptors[27]. Interestingly, 60-week-old HdhQ200 mice in the current study show a significant increase in striatal $GABA_A$ receptor binding, which does not appear at 80-week-old HdhQ200 mice [27]. In 80-week-old HdhQ200 mice, striatal $GABA_A$ receptor expression is essentially

identical to that of WT mice, despite marked reduction in striatal dopamine receptor expression. Stereologic analysis of 80-week-old HdhQ200 mice indicated no loss of neurons, suggesting that striatal neurotransmitter receptor changes result from dysregulation of receptor expression [27]. It is possible that abnormal upregulation of striatal $GABA_A$ receptor binding occurs in HdhQ200 mice, peaks prior to 80-weeks of age, and then declines with progressive dysfunction of striatal neurons. The increase in GABA receptor binding described here for HdhQ200 mice has been reported in human HD brain [51, 52] and R6/2 transgenic mice [53], but to our knowledge has not been similarly assessed in other knock-in models of HD.

The HdhQ200 mice used in this experiment, while derived from the mice used in the original characterization of this line [27] were raised in a different colony and evaluated by different personnel. The behavioral and pathologic results obtained in the current study are faithful to results obtained with the original characterization of this line. In addition, this study demonstrates reduced levels of Hsp70, suggesting that this HD knock-in mouse model recapitulates another likely feature of HD observed in an unrelated transgenic HD mouse model [28]. The stability of this model across laboratories emphasizes the usefulness of this line as a model of HD. We should add that HdhQ200 mice display a mild, age-dependent progressive phenotype and thus do not allow us to formally exclude a protective role for ataxin-3 early in disease pathogenesis, before HdhQ200 manifests behavioral signs of disease. Indeed some findings support a role for ataxin-3 during embryonic or early postnatal stages of life [24, 26, 54]. To assess the putative neuroprotective function of ataxin-3 at earlier ages, R6/2 transgenic mice, which develop a severe, rapidly progressive phenotype, may represent a good option.

In conclusion, our findings do not provide strong evidence that ataxin-3, a DUB implicated in protein quality control, modulates polyglutamine-induced disease in a knock-in mouse model of HD. These results suggest that ataxin-3 is not involved significantly in modulating cellular responses to mutant htt.

Acknowledgments

This work was supported by NIH NS038712 (HLP). We thank Randall N. Pittman for providing *Atxn3* knock-out mice, Peter J. Detloff for assistance with htt genotyping, Svetlana Fischer for assistance with immunohistochemical staining, Maria do Carmo Costa for assistance with behavioral tests.

References

1. Williams AJ, Paulson HL. Polyglutamine neurodegeneration: protein misfolding revisited. Trends Neurosci. Oct; 2008 31(10):521–8. PubMed PMID: 18778858. [PubMed: 18778858]
2. Orr HT, Zoghbi HY. Reversing neurodegeneration: a promise unfolds. Cell. Mar 31; 2000 101(1):1–4. PubMed PMID: 10778849. [PubMed: 10778849]
3. Paulson HL, Perez MK, Trottier Y, Trojanowski JQ, Subramony SH, Das SS, Vig P, Mandel JL, Fischbeck KH, Pittman RN. Intranuclear inclusions of expanded polyglutamine protein in spinocerebellar ataxia type 3. Neuron. Aug; 1997 19(2):333–44. PubMed PMID: 9292723. [PubMed: 9292723]
4. Paulson HL, Albin RL. Huntington's Disease: Clinical Features and Routes to Therapy. PubMed PMID: 21882418.
5. Clague MJ, Urbe S. Ubiquitin: same molecule, different degradation pathways. Cell. Nov 24; 2010 143(5):682–5. PubMed PMID: 21111229. [PubMed: 21111229]
6. Finkbeiner S, Mitra S. The ubiquitin-proteasome pathway in Huntington's disease. TheScientificWorldJournal. 2008; 8:421–33. PubMed PMID: 18454252. Pubmed Central PMCID: 2637619.

7. Kalchman MA, Graham RK, Xia G, Koide HB, Hodgson JG, Graham KC, Goldberg YP, Gietz RD, Pickart CM, Hayden MR. Huntingtin is ubiquitinated and interacts with a specific ubiquitin-conjugating enzyme. The Journal of biological chemistry. Aug 9; 1996 271(32):19385–94. PubMed PMID: 8702625. [PubMed: 8702625]
8. de Pril R, Fischer DF, Roos RA, van Leeuwen FW. Ubiquitin-conjugating enzyme E2-25K increases aggregate formation and cell death in polyglutamine diseases. Molecular and cellular neurosciences. Jan; 2007 34(1):10–9. PubMed PMID: 17092742. [PubMed: 17092742]
9. Yang H, Zhong X, Ballar P, Luo S, Shen Y, Rubinsztein DC, Monteiro MJ, Fang S. Ubiquitin ligase Hrd1 enhances the degradation and suppresses the toxicity of polyglutamine-expanded huntingtin. Experimental cell research. Feb 1; 2007 313(3):538–50. PubMed PMID: 17141218. [PubMed: 17141218]
10. Tsai YC, Fishman PS, Thakor NV, Oyler GA. Parkin facilitates the elimination of expanded polyglutamine proteins and leads to preservation of proteasome function. The Journal of biological chemistry. Jun 13; 2003 278(24):22044–55. PubMed PMID: 12676955. [PubMed: 12676955]
11. Miller VM, Nelson RF, Gouvion CM, Williams A, Rodriguez-Lebron E, Harper SQ, Davidson BL, Rebagliati MR, Paulson HL. CHIP suppresses polyglutamine aggregation and toxicity in vitro and in vivo. J Neurosci. Oct 5; 2005 25(40):9152–61. PubMed PMID: 16207874. [PubMed: 16207874]
12. Burnett B, Li F, Pittman RN. The polyglutamine neurodegenerative protein ataxin-3 binds polyubiquitylated proteins and has ubiquitin protease activity. Hum Mol Genet. Dec 1; 2003 12(23):3195–205. PubMed PMID: 14559776. [PubMed: 14559776]
13. Chai Y, Berke SS, Cohen RE, Paulson HL. Poly-ubiquitin binding by the polyglutamine disease protein ataxin-3 links its normal function to protein surveillance pathways. The Journal of biological chemistry. Jan 30; 2004 279(5):3605–11. PubMed PMID: 14602712. [PubMed: 14602712]
14. Scheel H, Tomiuk S, Hofmann K. Elucidation of ataxin-3 and ataxin-7 function by integrative bioinformatics. Hum Mol Genet. Nov 1; 2003 12(21):2845–52. PubMed PMID: 12944423. [PubMed: 12944423]
15. Todi SV, Winborn BJ, Scaglione KM, Blount JR, Travis SM, Paulson HL. Ubiquitination directly enhances activity of the deubiquitinating enzyme ataxin-3. The EMBO journal. Feb 18; 2009 28(4):372–82. PubMed PMID: 19153604. Pubmed Central PMCID: 2646149. [PubMed: 19153604]
16. Costa Mdo C, Paulson HL. Toward understanding Machado-Joseph disease. Progress in neurobiology. May; 2012 97(2):239–57. PubMed PMID: 22133674. Pubmed Central PMCID: 3306771. [PubMed: 22133674]
17. Jana NR, Dikshit P, Goswami A, Kotliarova S, Murata S, Tanaka K, Nukina N. Co-chaperone CHIP associates with expanded polyglutamine protein and promotes their degradation by proteasomes. The Journal of biological chemistry. Mar 25; 2005 280(12):11635–40. PubMed PMID: 15664989. [PubMed: 15664989]
18. Scaglione KM, Zavodszky E, Todi SV, Patury S, Xu P, Rodriguez-Lebron E, Fischer S, Konen J, Djarmati A, Peng J, Gestwicki JE, Paulson HL. Ube2w and ataxin-3 coordinately regulate the ubiquitin ligase CHIP. Molecular cell. Aug 19; 2011 43(4):599–612. PubMed PMID: 21855799. Pubmed Central PMCID: 3166620. [PubMed: 21855799]
19. Durcan TM, Kontogiannea M, Thorarinsdottir T, Fallon L, Williams AJ, Djarmati A, Fantaneanu T, Paulson HL, Fon EA. The Machado-Joseph disease-associated mutant form of ataxin-3 regulates parkin ubiquitination and stability. Hum Mol Genet. Jan 1; 2011 20(1):141–54. PubMed PMID: 20940148. Pubmed Central PMCID: 3005906. [PubMed: 20940148]
20. Winborn BJ, Travis SM, Todi SV, Scaglione KM, Xu P, Williams AJ, Cohen RE, Peng J, Paulson HL. The deubiquitinating enzyme ataxin-3, a polyglutamine disease protein, edits Lys63 linkages in mixed linkage ubiquitin chains. The Journal of biological chemistry. Sep 26; 2008 283(39): 26436–43. PubMed PMID: 18599482. Pubmed Central PMCID: 2546540. [PubMed: 18599482]
21. Zhong X, Pittman RN. Ataxin-3 binds VCP/p97 and regulates retrotranslocation of ERAD substrates. Hum Mol Genet. Aug 15; 2006 15(16):2409–20. PubMed PMID: 16822850. [PubMed: 16822850]

22. Burnett BG, Pittman RN. The polyglutamine neurodegenerative protein ataxin 3 regulates aggresome formation. Proceedings of the National Academy of Sciences of the United States of America. Mar 22; 2005 102(12):4330–5. PubMed PMID: 15767577. Pubmed Central PMCID: 555481. [PubMed: 15767577]

23. Warrick JM, Morabito LM, Bilen J, Gordesky-Gold B, Faust LZ, Paulson HL, Bonini NM. Ataxin-3 suppresses polyglutamine neurodegeneration in Drosophila by a ubiquitin-associated mechanism. Molecular cell. Apr 1; 2005 18(1):37–48. PubMed PMID: 15808507. [PubMed: 15808507]

24. Reina CP, Nabet BY, Young PD, Pittman RN. Basal and stress-induced Hsp70 are modulated by ataxin-3. Cell stress & chaperones. Nov; 2012 17(6):729–42. PubMed PMID: 22777893. Pubmed Central PMCID: 3468683. [PubMed: 22777893]

25. Schmitt I, Linden M, Khazneh H, Evert BO, Breuer P, Klockgether T, Wuellner U. Inactivation of the mouse Atxn3 (ataxin-3) gene increases protein ubiquitination. Biochem Biophys Res Commun. Oct 26; 2007 362(3):734–9. PubMed PMID: 17764659. [PubMed: 17764659]

26. Rodrigues AJ, do Carmo Costa M, Silva TL, Ferreira D, Bajanca F, Logarinho E, Maciel P. Absence of ataxin-3 leads to cytoskeletal disorganization and increased cell death. Biochimica et biophysica acta. Oct; 2010 1803(10):1154–63. PubMed PMID: 20637808. [PubMed: 20637808]

27. Heng MY, Duong DK, Albin RL, Tallaksen-Greene SJ, Hunter JM, Lesort MJ, Osmand A, Paulson HL, Detloff PJ. Early autophagic response in a novel knock-in model of Huntington disease. Hum Mol Genet. Oct 1; 2010 19(19):3702–20. PubMed PMID: 20616151. [PubMed: 20616151]

28. Hay DG, Sathasivam K, Tobaben S, Stahl B, Marber M, Mestril R, Mahal A, Smith DL, Woodman B, Bates GP. Progressive decrease in chaperone protein levels in a mouse model of Huntington's disease and induction of stress proteins as a therapeutic approach. Hum Mol Genet. Jul 1; 2004 13(13):1389–405. PubMed PMID: 15115766. [PubMed: 15115766]

29. Heng MY, Tallaksen-Greene SJ, Detloff PJ, Albin RL. Longitudinal evaluation of the Hdh(CAG)150 knock-in murine model of Huntington's disease. J Neurosci. Aug 22; 2007 27(34): 8989–98. PubMed PMID: 17715336. [PubMed: 17715336]

30. Tallaksen-Greene SJ, Crouse AB, Hunter JM, Detloff PJ, Albin RL. Neuronal intranuclear inclusions and neuropil aggregates in HdhCAG(150) knockin mice. Neuroscience. 2005; 131(4): 843–52. PubMed PMID: 15749339. [PubMed: 15749339]

31. Cemal CK, Carroll CJ, Lawrence L, Lowrie MB, Ruddle P, Al-Mahdawi S, King RH, Pook MA, Huxley C, Chamberlain S. YAC transgenic mice carrying pathological alleles of the MJD1 locus exhibit a mild and slowly progressive cerebellar deficit. Hum Mol Genet. May 1; 2002 11(9): 1075–94. PubMed PMID: 11978767. [PubMed: 11978767]

32. Cha JH, Kosinski CM, Kerner JA, Alsdorf SA, Mangiarini L, Davies SW, Penney JB, Bates GP, Young AB. Altered brain neurotransmitter receptors in transgenic mice expressing a portion of an abnormal human huntington disease gene. Proceedings of the National Academy of Sciences of the United States of America. May 26; 1998 95(11):6480–5. PubMed PMID: 9600992. Pubmed Central PMCID: 27817. [PubMed: 9600992]

33. Paulson, HL.; Albin, RL. Huntington's Disease: Clinical Features and Routes to Therapy.. Neurobiology of Huntington's Disease: Applications to Drug Discovery.. In: Lo, DC.; Hughes, RE., editors. Frontiers in Neuroscience. Boca Raton; FL: 2011.

34. Kettner M, Willwohl D, Hubbard GB, Rub U, Dick EJ Jr. Cox AB, Trottier Y, Auburger G, Braak H, Schultz C. Intranuclear aggregation of nonexpanded ataxin-3 in marinesco bodies of the nonhuman primate substantia nigra. Experimental neurology. Jul; 2002 176(1):117–21. PubMed PMID: 12093088. [PubMed: 12093088]

35. Fujigasaki H, Uchihara T, Takahashi J, Matsushita H, Nakamura A, Koyano S, Iwabuchi K, Hirai S, Mizusawa H. Preferential recruitment of ataxin-3 independent of expanded polyglutamine: an immunohistochemical study on Marinesco bodies. Journal of neurology, neurosurgery, and psychiatry. Oct; 2001 71(4):518–20. PubMed PMID: 11561037. Pubmed Central PMCID: 1763515.

36. Reina CP, Zhong X, Pittman RN. Proteotoxic stress increases nuclear localization of ataxin-3. Hum Mol Genet. Jan 15; 2010 19(2):235–49. PubMed PMID: 19843543. Pubmed Central PMCID: 2796889. [PubMed: 19843543]

37. Chafekar SM, Duennwald ML. Impaired heat shock response in cells expressing full-length polyglutamine-expanded huntingtin. PloS one. 2012; 7(5):e37929. PubMed PMID: 22649566. Pubmed Central PMCID: 3359295. [PubMed: 22649566]
38. Hubener J, Riess O. Polyglutamine-induced neurodegeneration in SCA3 is not mitigated by non-expanded ataxin-3: conclusions from double-transgenic mouse models. Neurobiology of disease. Apr; 2010 38(1):116–24. PubMed PMID: 20079840. [PubMed: 20079840]
39. Alves S, Nascimento-Ferreira I, Dufour N, Hassig R, Auregan G, Nobrega C, Brouillet E, Hantraye P, Pedroso de Lima MC, Deglon N, de Almeida LP. Silencing ataxin-3 mitigates degeneration in a rat model of Machado-Joseph disease: no role for wild-type ataxin-3? Hum Mol Genet. Jun 15; 2010 19(12):2380–94. PubMed PMID: 20308049. [PubMed: 20308049]
40. Todi SV, Paulson HL. Balancing act: deubiquitinating enzymes in the nervous system. Trends Neurosci. PubMed PMID. Jun 24.2011 :21704388. Pubmed Central PMCID: 3193880.
41. Seki T, Gong L, Williams AJ, Sakai N, Todi SV, Paulson HL. JosD1, a membrane-targeted deubiquitinating enzyme, is activated by ubiquitination and regulates membrane dynamics, cell motility and endocytosis. The Journal of biological chemistry. PubMed PMID. Apr 26.2013 : 23625928.
42. Weeks SD, Grasty KC, Hernandez-Cuebas L, Loll PJ. Crystal structure of a Josephin-ubiquitin complex: evolutionary restraints on ataxin-3 deubiquitinating activity. The Journal of biological chemistry. Feb 11; 2011 286(6):4555–65. PubMed PMID: 21118805. Pubmed Central PMCID: 3039388. [PubMed: 21118805]
43. Li F, Macfarlan T, Pittman RN, Chakravarti D. Ataxin-3 is a histone-binding protein with two independent transcriptional corepressor activities. The Journal of biological chemistry. Nov 22; 2002 277(47):45004–12. PubMed PMID: 12297501. [PubMed: 12297501]
44. Evert BO, Araujo J, Vieira-Saecker AM, de Vos RA, Harendza S, Klockgether T, Wullner U. Ataxin-3 represses transcription via chromatin binding, interaction with histone deacetylase 3, and histone deacetylation. J Neurosci. Nov 1; 2006 26(44):11474–86. PubMed PMID: 17079677. [PubMed: 17079677]
45. Chai Y, Wu L, Griffin JD, Paulson HL. The role of protein composition in specifying nuclear inclusion formation in polyglutamine disease. The Journal of biological chemistry. Nov 30; 2001 276(48):44889–97. PubMed PMID: 11572863. [PubMed: 11572863]
46. Araujo J, Breuer P, Dieringer S, Krauss S, Dorn S, Zimmermann K, Pfeifer A, Klockgether T, Wuellner U, Evert BO. FOXO4-dependent upregulation of superoxide dismutase-2 in response to oxidative stress is impaired in spinocerebellar ataxia type 3. Hum Mol Genet. Aug 1; 2011 20(15): 2928–41. PubMed PMID: 21536589. [PubMed: 21536589]
47. Hartl FU, Hayer-Hartl M. Molecular chaperones in the cytosol: from nascent chain to folded protein. Science. Mar 8; 2002 295(5561):1852–8. PubMed PMID: 11884745. [PubMed: 11884745]
48. Wacker JL, Huang SY, Steele AD, Aron R, Lotz GP, Nguyen Q, Giorgini F, Roberson ED, Lindquist S, Masliah E, Muchowski PJ. Loss of Hsp70 exacerbates pathogenesis but not levels of fibrillar aggregates in a mouse model of Huntington's disease. J Neurosci. Jul 15; 2009 29(28): 9104–14. PubMed PMID: 19605647. Pubmed Central PMCID: 2739279. [PubMed: 19605647]
49. Ferrante RJ. Mouse models of Huntington's disease and methodological considerations for therapeutic trials. Biochimica et biophysica acta. Jun; 2009 1792(6):506–20. PubMed PMID: 19362590. Pubmed Central PMCID: 2693467. [PubMed: 19362590]
50. Heng MY, Detloff PJ, Albin RL. Rodent genetic models of Huntington disease. Neurobiology of disease. Oct; 2008 32(1):1–9. PubMed PMID: 18638556. [PubMed: 18638556]
51. Glass M, Dragunow M, Faull RL. The pattern of neurodegeneration in Huntington's disease: a comparative study of cannabinoid, dopamine, adenosine and GABA(A) receptor alterations in the human basal ganglia in Huntington's disease. Neuroscience. 2000; 97(3):505–19. PubMed PMID: 10828533. [PubMed: 10828533]
52. Kunig G, Leenders KL, Sanchez-Pernaute R, Antonini A, Vontobel P, Verhagen A, Gunther I. Benzodiazepine receptor binding in Huntington's disease: [11C]flumazenil uptake measured using positron emission tomography. Annals of neurology. May; 2000 47(5):644–8. PubMed PMID: 10805336. [PubMed: 10805336]

53. Cepeda C, Starling AJ, Wu N, Nguyen OK, Uzgil B, Soda T, Andre VM, Ariano MA, Levine MS. Increased GABAergic function in mouse models of Huntington's disease: reversal by BDNF. Journal of neuroscience research. Dec 15; 2004 78(6):855–67. PubMed PMID: 15505789. [PubMed: 15505789]

54. do Carmo Costa M, Bajanca F, Rodrigues AJ, Tome RJ, Corthals G, Macedo-Ribeiro S, Paulson HL, Logarinho E, Maciel P. Ataxin-3 plays a role in mouse myogenic differentiation through regulation of integrin subunit levels. PloS one. 2010; 5(7):e11728. PubMed PMID: 20668528. Pubmed Central PMCID: 2909204. [PubMed: 20668528]

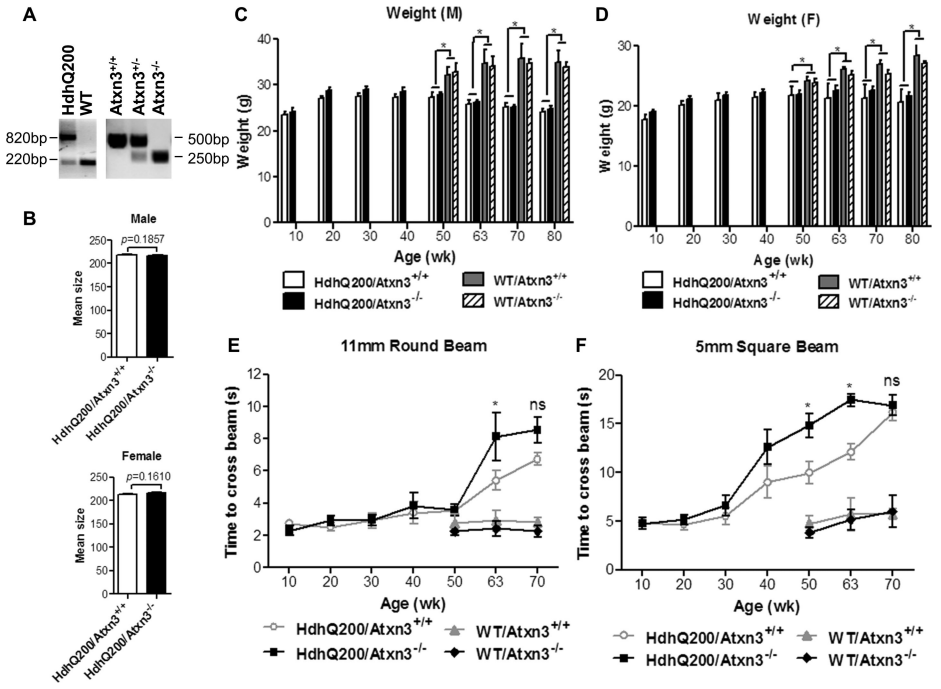

Fig.1. Loss of ataxin-3 has only modest effects on the behavioral phenotype of HdhQ200 mice

A) Mouse tail DNA was analyzed by PCR to determine genotype. HdhQ200-specific primers yield 820 and 220 bp fragment from HdhQ200 knock-in and wild type alleles, respectively. Ataxin-3 specific primers produce 500 and 250 bp fragments from ataxin-3 WT and null alleles, respectively.

B) CAG repeat size determination for HdhQ200/Atxn3$^{+/+}$ and HdhQ200/Atxn3$^{-/-}$ male mice (n= 19 and 11, respectively) and female mice (n= 18 and 15, respectively).

C, D) By 50 wks, HdhQ200 mice exhibit significant weight loss in both males and females, but deletion of ataxin-3 does not affect body weight in male or female HD mice.

E, F) Upon aging, HdhQ200 mice are slower to traverse balance beams, and deletion of ataxin-3 modestly increases this latency to transverse 11 mm round and 5 mm square beams. Results are mean ± SEM, and *p<0.05.

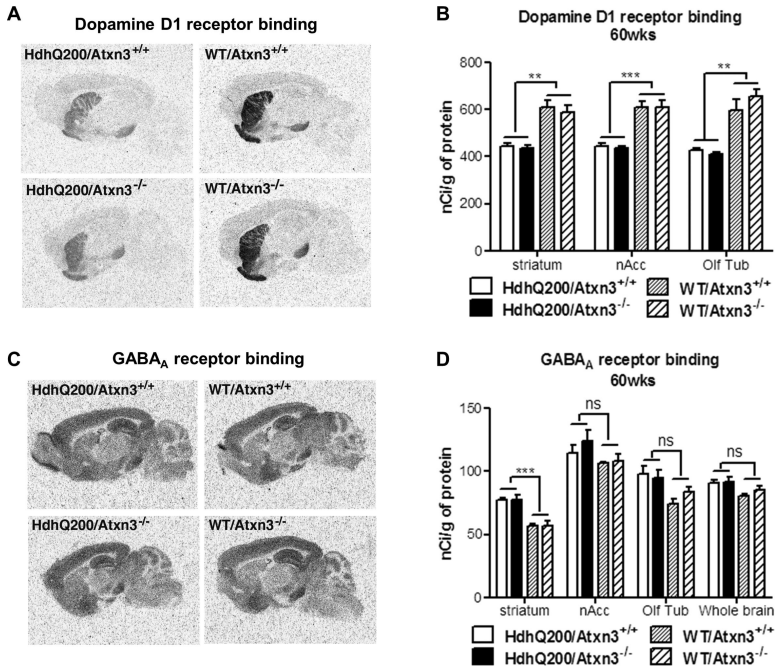

Fig.2. Deletion of ataxin-3 does not alter age-dependent changes in neurotransmitter receptor expression in HdhQ200 mice

Littermates from all four genotypes (n=4/group) were assessed at 60 weeks of age for expression of specific neurotransmitter receptors in different brain regions, measured by autoradiography. As previously reported [27], compared to wild type mice HdhQ200 mice show a significant decrease in D1 receptor binding in striatum, nuclear accumbens (nAcc) and olfactory tubercle (Olf Tub). A significant increase in striatal $GABA_A$ receptor binding in HdhQ200 mice has not been previously reported. One-way ANOVA with Bonferroni post hoc established that D1 receptor (A, B), D2 receptor (data not shown) and $GABA_A$ receptor (C, D) expression does not differ significantly between HdhQ200/$Atxn3^{+/+}$ and HdhQ200/$Atxn3^{-/-}$ mice. Error bars represent SEM. *p<0.05, **p<0.01, ***p<0.001 and ns = no significance.

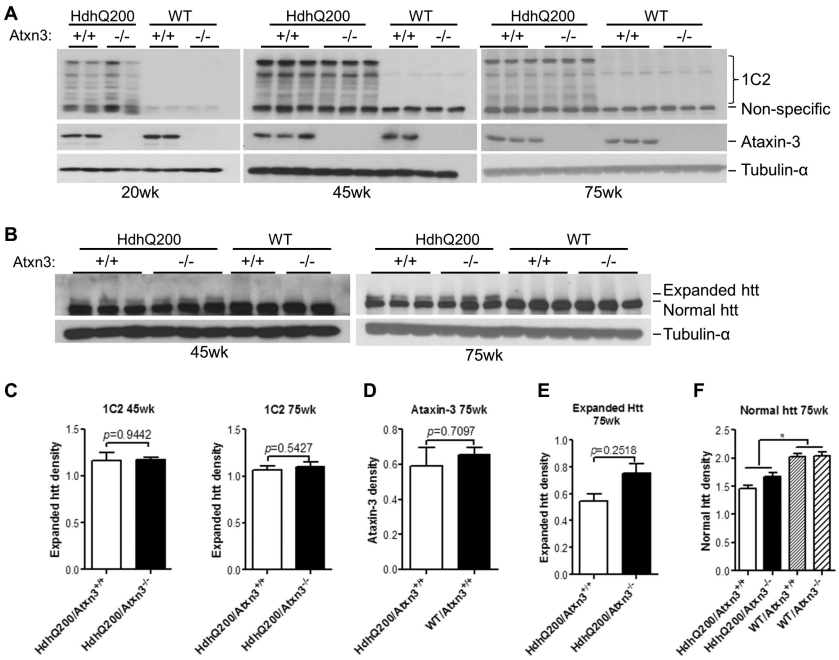

Fig.3. Deletion of ataxin-3 does not increase levels of mutant or normal htt in HdhQ200 mice

Forebrain homogenates from mice 20, 45 or 75 weeks of age were analyzed by western blot with A) anti-polyglutamine (1C2) and B) anti-htt2166 antibodies. 1C2 preferentially recognizes expanded polyglutamine-containing mutant htt whereas anti-htt2166 antibody recognizes both normal and expanded htt. Ataxin-3 expression in A is detected with 1H9 mAb, and tubulin-α was assessed as a loading control. Band intensities were quantified with ImageJ. Results in C-F represent means ± SEM. *$p<0.05$.

A, C) The expression of full length mutant htt (top band) and its various fragments detected with 1C2 does not differ significantly between HdhQ200/Atxn3$^{+/+}$ and HdhQ200/Atxn3$^{-/-}$ at 20, 45 and 75 weeks of age. Two-paired *t*-test (n=3).

A, D) Expression levels of ataxin-33 does not differ significantly between WT/Atxn3$^{+/+}$ and HdhQ200/Atxn3$^{+/+}$. In *Atxn3* null mice, the ataxin-3 protein is no longer detectable in brain lysate.

B, E, F) Deletion of ataxin-3 does not alter the levels of normal or expanded htt at 45 and 75 weeks of age. Normal htt levels, however, are slightly decreased in HdhQ200 mice (E, Two-paired *t*-test, n=3; F, one-way ANOVA, n=3).

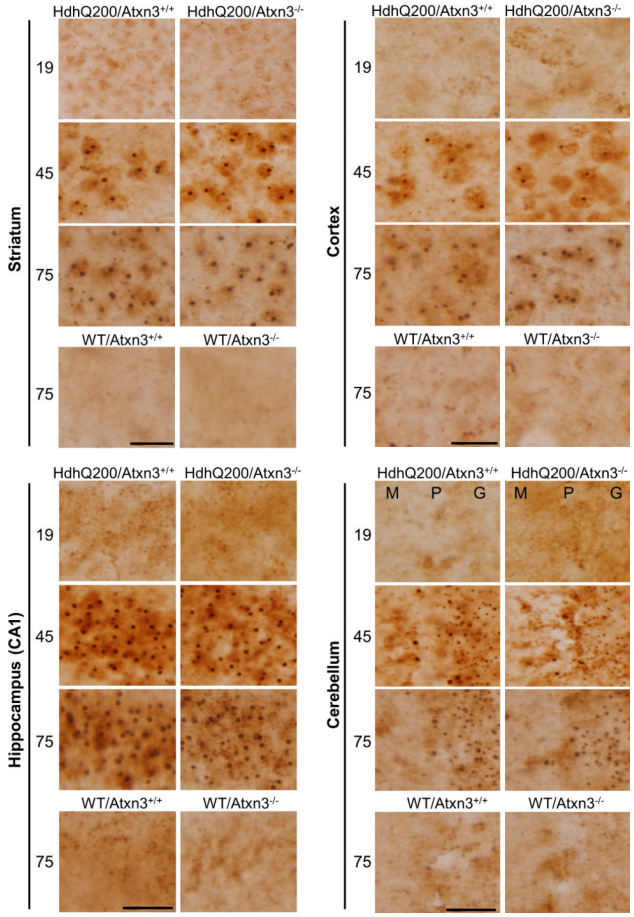

Fig.4. Loss of ataxin-3 does not alter inclusion body formation

Immunohistochemistry with an N-terminal htt antibody was performed on brain sections from 19, 45 and 75 week old mice (n=3 per genotype). HdhQ200 mice show age-dependent accumulation of inclusion bodies in various brain regions (striatum, cortex, hippocampus and cerebellum). The size and density of inclusion bodies were similar in HdhQ200 mice with or without ataxin-3. Scale bars =20 μm. M (Molecular layer), P (Purkinje cell layer), G (Granule cell layer).

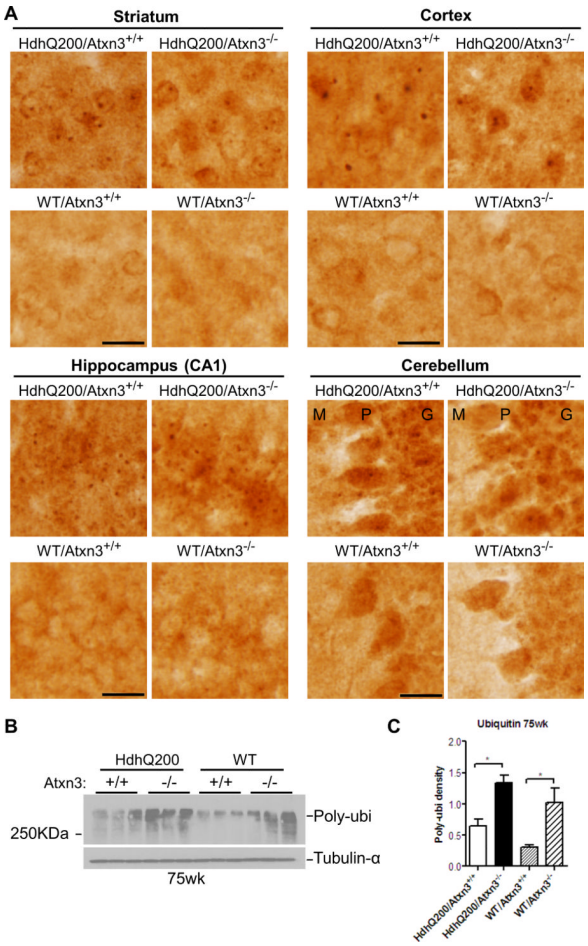

Fig.5. Deletion of ataxin-3 does not alter ubiquitination of htt inclusions, but increases total ubiquitinated proteins in wild type and HD mouse brain

A) Anti-ubiquitin immunohistochemistry on brain sections from 75 week old HD mice (n=3 per genotype) show robust and abundant ubiquitinated inclusions in various brain regions (striatum, cortex, hippocampus and cerebellum), regardless of the presence or absence of ataxin-3. Scale bars =20 μm. M (Molecular layer), P (Purkinje cell layer), G (Granule cell layer).

B-C) Levels of total ubiquitinated proteins in forebrain of 75-week-old mice, determined by western blot, Show that loss of ataxin-3 significantly increased levels of ubiqutinated proteins in forebrain. Results are means ± SEM, * $p<0.05$. Blots were quantified with ImageJ (One-way ANOVA followed by post hoc test, n=3)

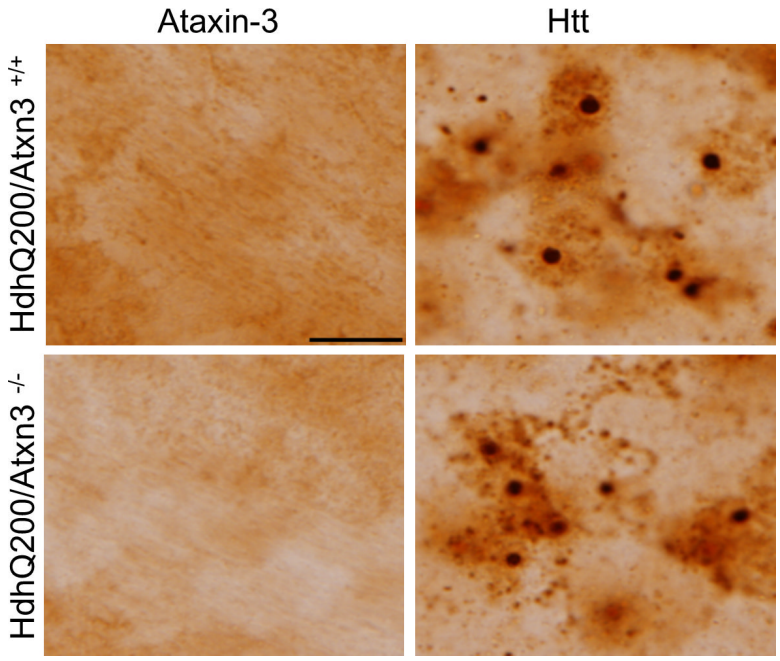

Fig.6. Ataxin-3 is not detectably recruited into htt inclusions

Representative images in the striatum of indicated genotypes immunostained with anti-ataxin-3 (1H9) antibody or anti-N terminal htt antibody. Scale bar =10 μm.

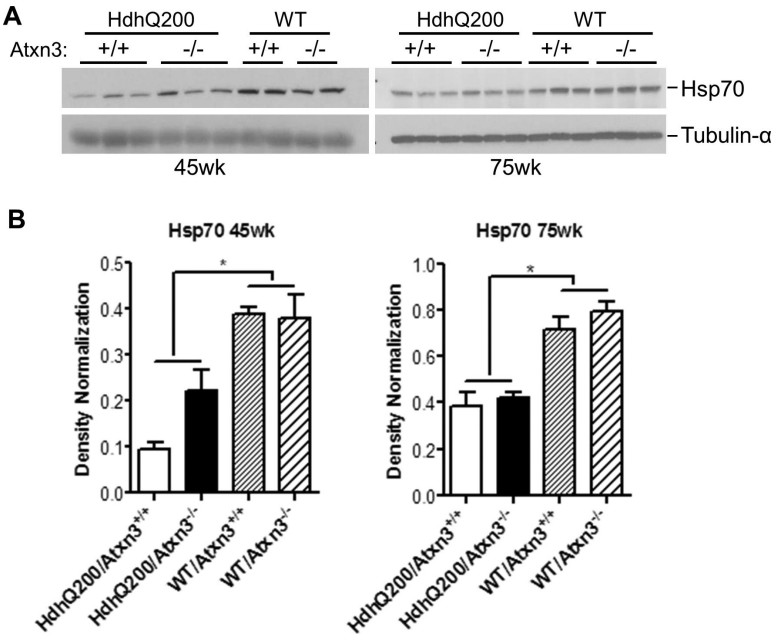

Fig.7. Hsp70 levels are decreased in the CNS of HD mice but are not further altered by deletion of ataxin-3

A) Forebrain homogenates aged 45 and 75 weeks were analyzed by western blot with hsp70 antibody.

B-C) Levels of Hsp70 are lower in HdhQ200 mice than in WT mice, and this difference is not affected by the presence or absence of ataxin-3. Results are means ± SEM (Oneway ANOVA, n=3, * $p<0.05$)

Table 1A

Inclusion body number in 45 week old HdhQ200 mice

	Striatum	Cortex	Hippocampus	Cerebellum
HdhQ200/Atxn3$^{+/+}$	103±4(3)	106±9(3)	139±4(3)	537±28(3)
HdhQ200/Atxn3$^{-/-}$	105±4(3)	109±5(3)	149±4(3)	590±13(3)
P value	0.6876	0.2661	0.0881	0.0945

Table 1B

Inclusion body size in 45 week old HdhQ200 mice

	Striatum	**Cortex**	**Hippocampus**	**Cerebellum**
HdhQ200/Atxn3$^{+/+}$	1072±85(3)	958±86(3)	821±28(3)	237±4(3)
HdhQ200/Atxn3$^{-/-}$	1078±24(3)	1014±38(3)	737±20(3)	229±8(3)
P value	0.9016	0.5923	0.1137	0.3530

Table 1C

Inclusion body number in 75 week old HdhQ200 mice

	Striatum	Cortex	Hippocampus	Cerebellum
HdhQ200/Atxn3$^{+/+}$	124±9(4)	140±11(4)	182±6(4)	641±10(4)
HdhQ200/Atxn3$^{-/-}$	127±7(4)	129±5(4)	203±7(4)	692±29(4)
P value	0.7746	0.4505	0.1768	0.2159

Table 1D

Inclusion body size at 75 week old HdhQ200 mice

	Striatum	Cortex	Hippocampus	Cerebellum
HdhQ200/Atxn3$^{+/+}$	1266±41(4)	1263±95(4)	1055±25(4)	323±38(4)
HdhQ200/Atxn3$^{-/-}$	1242±46(4)	1229±70(4)	1004±29(4)	286±13(4)
P value	0.6983	0.3606	0.1817	0.0553

All values are the mean ± SEM. The *n* is indicated in parentheses.